

ChemComm

Accepted Manuscript



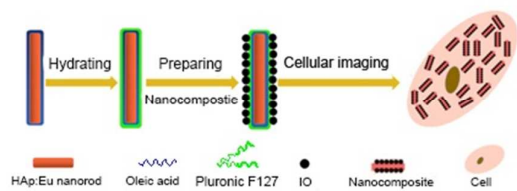
This is an *Accepted Manuscript*, which has been through the Royal Society of Chemistry peer review process and has been accepted for publication.

Accepted Manuscripts are published online shortly after acceptance, before technical editing, formatting and proof reading. Using this free service, authors can make their results available to the community, in citable form, before we publish the edited article. We will replace this *Accepted Manuscript* with the edited and formatted *Advance Article* as soon as it is available.

You can find more information about *Accepted Manuscripts* in the [Information for Authors](#).

Please note that technical editing may introduce minor changes to the text and/or graphics, which may alter content. The journal's standard [Terms & Conditions](#) and the [Ethical guidelines](#) still apply. In no event shall the Royal Society of Chemistry be held responsible for any errors or omissions in this *Accepted Manuscript* or any consequences arising from the use of any information it contains.

A table of contents entry



Fluorescent-magnetic iron oxide coated fluoridated HAp/Ln³⁺ (Ln=Eu or Tb) nanocomposites were prepared for cellular imaging.

Cite this: DOI: 10.1039/c0xx00000x

www.rsc.org/xxxxxx

COMMUNICATION

Synthesis of Iron Oxide coated Fluoridated HAp/Ln³⁺ (Ln=Eu or Tb) nanocomposites for Biological Applications

Jie Pan,^{a*} Juchen Zhang,^a Lili Wang,^a Dong Wan^{a*}

Received (in XXX, XXX) Xth XXXXXXXXXX 20XX, Accepted Xth XXXXXXXXXX 20XX

DOI: 10.1039/b000000x

Fluorescent-magnetic iron oxide coated fluoridated HAp/Ln³⁺ (Ln=Eu or Tb) nanocomposites were prepared. After transforming hydrophobic fluoridated HAp/Ln³⁺ nanorods into hydrophilic ones, iron oxide particles were coated on their surface via thermal decomposition of Fe(acac)₃. Fluorescent-magnetic nanocomposites developed in this study demonstrate excellent fluorescent-magnetic properties and prominent biocompatibility.

Fluorescent-magnetic nanocomposites can be used widely for a great deal of biological areas.¹⁻⁹ It is well known that hydroxyapatite (HAp) is the main inorganic component of bones and teeth of humans and animals; therefore HAp has excellent biocompatibility and biodegradability.¹⁰⁻²¹ In 2012, Hui *et al.* exploited a hydrothermal approach to dope rare earth with fluorine ions to fabricate fluoridated HAp nanocrystals with excellent luminescent properties and high biocompatibility.²¹ Therefore, Ln³⁺ ion doped HAp nanoparticles are quite suitable to fabricate fluorescent-magnetic nanocomposites for biological applications.²¹

In this study, new fluorescent-magnetic nanocomposites were prepared through coating iron oxide on the surface of fluoridated HAp (FHAp)/Ln³⁺ nanorods. Briefly, hydrophobic FHAp/Eu³⁺ (or Tb³⁺) nanorods were firstly fabricated. Next, a surfactant of Pluronic F127 was adopted to convert hydrophobic FHAp/Eu³⁺ (or Tb³⁺) nanorods into hydrophilic ones. Furthermore, fluorescent-magnetic nanocomposites of iron oxide coated FHAp/Eu³⁺ (or Tb³⁺) nanorods were fabricated through thermal decomposition of Iron (III) acetylacetonate (Fe(acac)₃) in triethylene glycol (TEG) on the surface of FHAp/Eu³⁺ (or Tb³⁺) nanorods. Moreover, the experiments about characterization, photoluminescence and magnetic of nanocomposites were carried out. Finally, the *in vitro* cytotoxicity and cellular imaging of nanocomposites were investigated. The findings in this study demonstrated that nanocomposites developed in this study show unique fluorescent-magnetic properties and excellent biocompatibility.

As described in the experimental section, thermal decomposition of Fe(acac)₃ was adopted to fabricate nanocomposites. Figure 1 presents the detailed scheme about the preparation of nanocomposites for cellular imaging. It was reported that the formational mechanism of iron oxide coated FHAp/Eu³⁺ (or Tb³⁺) nanocomposites was speculated as following.^{22,23} After Fe(acac)₃ were decomposed, some of them were reduced by TEG into

magnetite tiny particles with high surface energy, which were preferentially adsorbed onto the surface of FHAp/Eu³⁺ (or Tb³⁺) nanorods. Due to the interaction of van der Waals forces and magnetic dipole, these magnetite tiny particles can grow slightly. Once these magnetite tiny particles grew to reach a critical size, they were stabilized with TEG. Consequently, iron oxide particles were decorating on the surface of FHAp/Eu³⁺ (or Tb³⁺) nanorods to form nanocomposites.

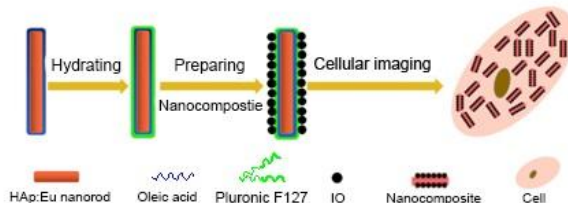


Fig. 1 Scheme showing the synthesis of iron oxide coated FHAp/Eu³⁺ (or Tb³⁺) nanocomposites and their used for cell imaging.

Figure 2a illustrates the transmission electron microscopy (TEM) images of hydrophobic FHAp/Eu³⁺ nanorods. It can be noticed in figure 1a that hydrophobic nanorods are a well-defined rod shape with homogeneously distributed around 150 nm in length. Furthermore, the surfactant of Pluronic F127 was used to modify the surface of hydrophobic FHAp/Eu³⁺ nanorods in order to transform hydrophobic nanorods into hydrophilic ones. As shown in figure 2b, hydrophilic FHAp/Eu³⁺ nanorods are still keep good rod shape with uniform in size, which indicate that the surface modification of hydrophobic FHAp/Eu³⁺ nanorods with Pluronic F127 did not seem to cause morphological changes. Moreover, The TEM images of three nanocomposites at different mass ratio of FHAp/Eu³⁺ nanorods and iron oxide (5:1, 2:1 and 1:1) fabricated under same experimental conditions were shown in figure 2c, 2d, and 2e, respectively. High resolution transmission electron microscopy (HRTEM) image shown in figure 2f further reveals obviously that the successful decoration of iron oxide on the surface of FHAp/Eu³⁺ nanorods. Interestingly, as shown in figure 2f, these tiny iron oxide particles on the surface of nanocomposite were distributed uniformly.

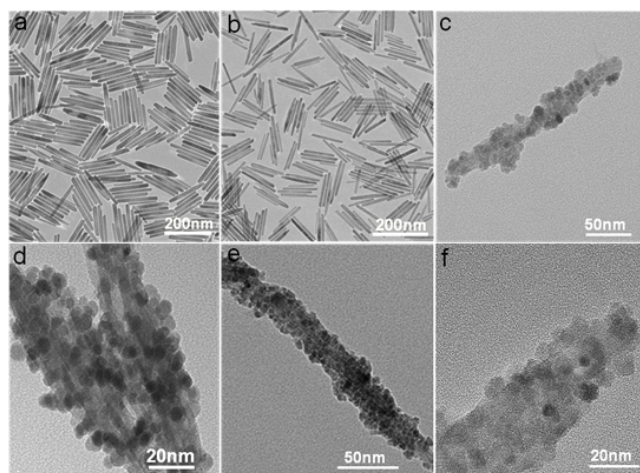


Fig. 2 a) TEM images of hydrophobic FHAp/ Eu³⁺ nanorods; b) TEM images of hydrophilic FHAp/ Eu³⁺ nanorods; c), d) and e) TEM images of nanocomposite at different mass ratio of FHAp/Eu³⁺ nanorods and iron oxide (5:1, 2:1 and 1:1); f) a high resolution TEM image of IO-Eu-FHAp (FHAp/ Eu³⁺: IO = 2:1)

Figure 3 shown XRD pattern of the IO-Eu-FHAp (FHAp/Eu³⁺: IO = 2:1). This XRD displays that there is only FHAp/Eu³⁺ and iron oxide appeared in the final products, which confirmed that iron oxide has been successfully decorated on the surface of FHAp/Eu³⁺ nanorods.

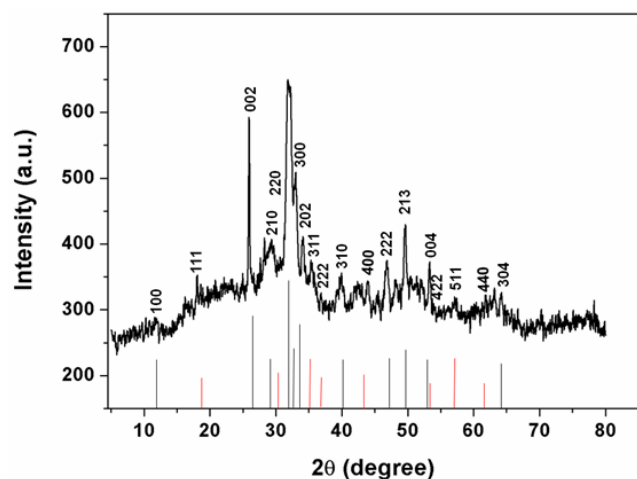


Fig.3 XRD pattern of the IO-Eu-FHAp (FHAp/ Eu³⁺: IO = 2:1).

It was shown in figure 4a) the emission spectrum of the IO-Eu-FHAp (FHAp/ Eu³⁺: IO = 2:1) in water at 405 nm excitation and b) emission spectrum of IO-Tb-FHAp (FHAp/ Tb³⁺: IO = 2:1) in water at 488 nm excitation. From this figure, it can be seen that the main emission peaks appear in 674 nm for IO-Eu-FHAp and 539 nm for IO-Tb-FHAp, respectively. Importantly, these nanorods kept well stable so that strong fluorescence could still be detected after stored about a month. Above findings implied these nanocomposites have excellent luminescent properties and stable in aqueous solutions, which are suitable for cellular imaging.

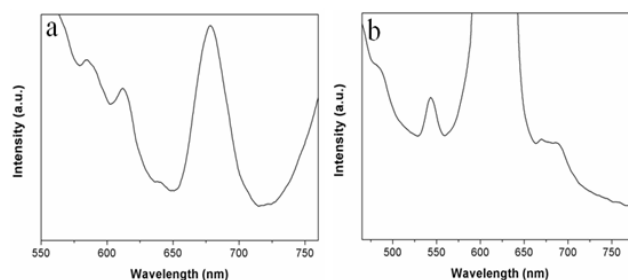


Fig.4 a) The emission spectrum of the IO-Eu-FHAp (FHAp/ Eu³⁺: IO = 2:1) in water at 405 nm excitation; b) the emission spectrum of IO-Tb-FHAp (FHAp/ Tb³⁺: IO = 2:1) in water at 488 nm excitation.

Iron oxide particles were coated on the surface of FHAp/Ln³⁺ nanorods to enable them magnetic. A vibrating sample magnetometer (VSM) was used to analyze the magnetic properties of nanocomposites. Figure 5 illustrated room-temperature hysteresis curve of the IO-Eu-FHAp (FHAp/Eu³⁺: IO = 2:1). The amount of magnetization of nanocomposites was shown against the varying magnetic field. The saturation magnetizations were determined to be 4.8 emu/g of iron oxide for nanocomposites, which indicate that the supraparamagnetic property of the iron oxide particles in the nanocomposites is remain, which makes these nanocomposites be promising tools for the current and potential biomedical applications such as biological imaging, cell tracking, magnetic bioseparation, and so on.

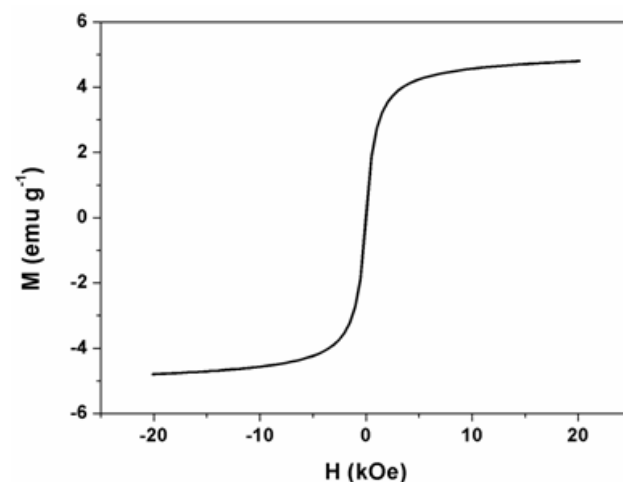


Fig.5 Room-temperature hysteresis curve of the IO-Eu-FHAp (FHAp/Eu³⁺: IO = 2:1).

In order to apply IO-Ln-FHAp for biological field, their cytotoxicity must be examined using CCK-8 assay. It is shown in Figure 6 that for A549 cells incubated with IO-Ln-FHAp (FHAp/Ln³⁺: IO = 2:1) at 0, 20, 40, 80, 150 and 300 μg mL⁻¹ nanocomposites concentration for 8 h and 24 h, the resulting of cell viability displays low cytotoxicity of nanocompositions to A549 cells. Their cell viability values were still greater than 90% even at 300 μg mL⁻¹ of nanocomposites concentration, which further confirms the low toxicity of nanocomposites. These nanocompositions should thus be promising tools for various biological applications.

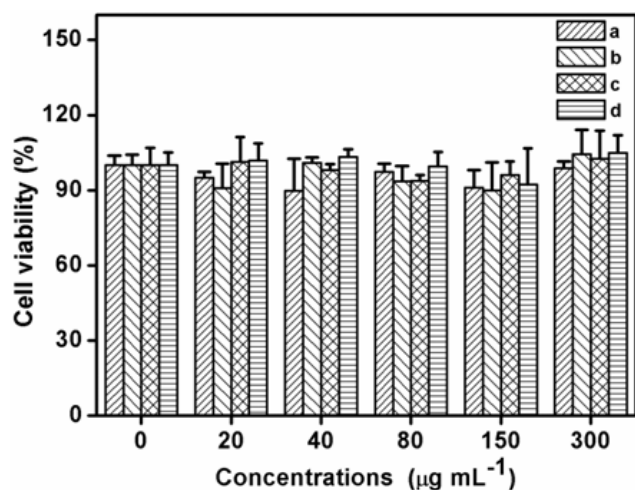


Fig.6 CCK-8 assay of A549 cells cultured at different nanocomposites concentrations with: a) IO-Eu-FHAp (FHAp/ Eu^{3+} : IO = 2:1) for 8 h; b) IO-Tb-FHAp (FHAp/ Tb^{3+} : IO = 2:1) for 8 h; c) IO-Eu-FHAp (FHAp/ Eu^{3+} : IO = 2:1) for 24 h; d) IO-Tb-FHAp (FHAp/ Tb^{3+} : IO = 2:1) for 24 h.

IO-Ln-FHAp applied for cellular imaging were examined to demonstrate the penetration of the nanocomposites into the cells with CLSM. In figure 7, the images in figure 7B obtained from the red channel which demonstrates the red fluorescence of IO-Eu-FHAp (FHAp/ Eu^{3+} : IO = 2:1); the images in figure 7E obtained from the green channel which shows the green fluorescence of IO-Tb-FHAp (FHAp/ Tb^{3+} : IO = 2:1). It can be seen in figure 7 that the nanocomposites were internalized in the cytoplasm around cell nucleus, which confirms nanocomposites can be used efficiently for cellular imaging.

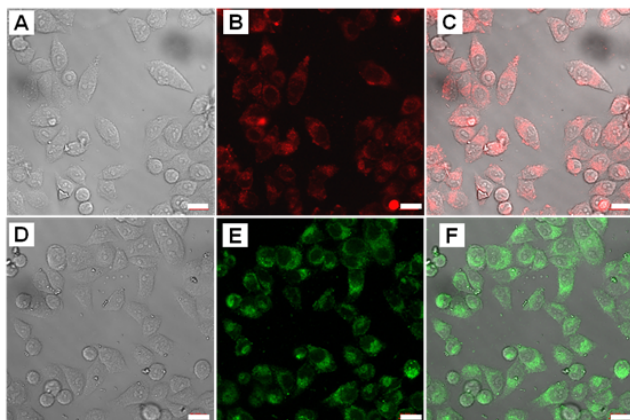


Fig.7 CLSM images of A549 cells after 4 h incubation in medium with $250 \mu\text{g mL}^{-1}$ nanocomposites: A-C) IO-Eu-FHAp (FHAp/ Eu^{3+} : IO = 2:1); D-F) IO-Tb-FHAp (FHAp/ Tb^{3+} : IO = 2:1). Left column show bright fields; B) red fluorescent image excited at 405 nm; E) green fluorescent image excited at 488 nm; images in right column obtained by combination of the left and middle column. Scale bar = 20 μm .

Conclusions

IO-Ln-FHAp with fluoresce and magnetism were successfully developed in this study through thermal decomposition of $\text{Fe}(\text{acac})_3$ in triethylene glycol (TEG) on the surface of FHAp/ Ln^{3+} nanorods. These 'two-in-one' fluorescent-magnetic nanocomposites demonstrate excellent biocompatibility and the properties of photoluminescence and magnetic, which enable

them be utilized in various biological fields. It can be expected in the future that these nanocomposites fabricated in this study will play import roles in biological applications.

This work was supported by the open funds from the key laboratory of biomedical materials in Tianjin, National Natural Science Foundation of China (91127040, 20921001, 21106101 and 21172171), 973 program (2011CB933100, 2011CB932402), Natural Science Foundation of Tianjin (11JCZDJC22300, 12JCZDJC29500 and 13JCONJC06300) and Ningbo Natural Science Foundation (2013A610085).

Notes and references

- ^a State Key Laboratory of Hollow Fiber Membrane Materials and Processes, School of Environmental and Chemical Engineering, Tianjin Polytechnic University, Tianjin 300387, P. R. China. panjie@tjpu.edu.cn; wandong_tjpu@126.com
- [†] Electronic Supplementary Information (ESI) available: [details of materials and methods were provided in supporting information]. See DOI: 10.1039/b000000x/
- H. W. Gu, K. M. Xu, Z. M. Yang, C. K. Chang and B. Xu, *Chemical Communications*, 2005, 4270-4272.
- B. Zebli, A. S. Susha, G. B. Sukhorukov, A. L. Rogach and W. J. Parak, *Langmuir*, 2005, **21**, 4262-4265.
- O. Veiseh, C. Sun, J. Gunn, N. Kohler, P. Gabikian, D. Lee, N. Bhattarai, R. Ellenbogen, R. Sze, A. Hallahan, J. Olson and M. Q. Zhang, *Nano Letters*, 2005, **5**, 1003-1008.
- H. Choi, S. R. Choi, R. Zhou, H. F. Kung and I. W. Chen, *Academic Radiology*, 2004, **11**, 996-1004.
- L. Cheng, K. Yang, Y. G. Li, X. Zeng, M. W. Shao, S. T. Lee and Z. Liu, *Biomaterials*, 2012, **33**, 2215-2222.
- O. Veiseh, J. W. Gunn and M. Q. Zhang, *Advanced Drug Delivery Reviews*, 2010, **62**, 284-304.
- S. Takeda, F. Mishima, S. Fujimoto, Y. Izumi and S. Nishijima, *Journal of Magnetism and Magnetic Materials*, 2007, **311**, 367-371.
- M. Arruebo, R. Fernandez-Pacheco, M. R. Ibarra and J. Santamaria, *Nano Today*, 2007, **2**, 22-32.
- B. Chertok, B. A. Moffat, A. E. David, F. Yu, C. Bergemann, B. D. Ross and V. C. Yang, *Biomaterials*, 2008, **29**, 487-496.
- L. C. Palmer, C. J. Newcomb, S. R. Kaltz, E. D. Spoerke and S. I. Stupp, *Chemical Reviews*, 2008, **108**, 4754-4783.
- C. M. Curtin, G. M. Cunniffe, F. G. Lyons, K. Bessho, G. R. Dickson, G. P. Duffy and F. J. O'Brien, *Advanced Materials*, 2012, **24**, 749-+.
- J. Hui and X. Wang, *Chemistry-a European Journal*, 2011, **17**, 6926-6930.
- J. Hui and X. Wang, *Inorganic Chemistry Frontiers*, 2014, **1**, 215-225.
- F. Chen, P. Huang, Y.-J. Zhu, J. Wu, C.-L. Zhang and D.-X. Cui, *Biomaterials*, 2011, **32**, 9031-9039.
- C. S. Ciobanu, S. L. Iconaru, F. Massuyeau, L. V. Constantin, A. Costescu and D. Predoi, *Journal of Nanomaterials*, 2012.
- O. A. Graeve, R. Kanakala, A. Madadi, B. C. Williams and K. C. Glass, *Biomaterials*, 2010, **31**, 4259-4267.
- Y. Han, X. Wang, H. Dai and S. Li, *Journal of Luminescence*, 2013, **135**, 281-287.
- K. Hasna, S. S. Kumar, M. Komath, M. R. Varma, M. K. Jayaraj and K. R. Kumar, *Physical Chemistry Chemical Physics*, 2013, **15**, 8106-8111.
- M. Liu, H. Liu, S. Sun, X. Li, Y. Zhou, Z. Hou and J. Lin, *Langmuir*, 2014, **30**, 1176-1182.
- J. Pan, D. Wan, Y. Bian, H. Sun, C. Zhang, F. Jin, Z. Huang and J. Gong, *Aiche Journal*, 2013, **59**, 4494-4501.
- J. Hui, X. Zhang, Z. Zhang, S. Wang, L. Tao, Y. Wei and X. Wang, *Nanoscale*, 2012, **4**, 6967-6970.
- H.-P. Cong, J.-J. He, Y. Lu and S.-H. Yu, *Small*, 2010, **6**, 169-173.
- J. Wan, W. Cai, J. Feng, X. Meng and E. Liu, *Journal of Materials Chemistry*, 2007, **17**, 1188-1192.